Quantum wire as a charge-qubit detector

Tomasz Kwapiński* and Ryszard Taranko†
Institute of Physics, Marie Curie-Skłodowska University, 20-031 Lublin, Poland
(Received 3 July 2012; revised manuscript received 30 October 2012; published 30 November 2012)

We present a proposal for a qubit charge meter (detector) based on a linear wire of quantum dots placed between two electron reservoirs. A qubit formed by an excess electron in a double quantum dot is coupled electrostatically with a single wire site and the dynamics of this system is studied using the equation of motion for appropriate correlation functions and the evolution operator method. For the qubit-wire system, depending on the qubit position on the wire the readout current oscillates over a long time or the current oscillations decrease very rapidly. This effect cannot be explained in terms of different charges of the wire sites (the same occupancies of all sites are considered). We have found that the qubit's decoherence strongly depends on the structure of the local density of states of the site which is coupled with the qubit. Additionally, the period of the readout current oscillations changes with the wire-qubit electrostatic coupling.

DOI: 10.1103/PhysRevA.86.052338 PACS number(s): 03.67.Lx, 05.60.Gg, 73.23.−b, 73.63.Nm

I. INTRODUCTION

The basic blocks of quantum computers are qubits (two-state systems). One of the most popular realizations of qubits represents two coupled quantum dots (QDs). Such a double-quantum-dot (DQD) system with one excess electron forms a charge qubit. Decoherence of the qubit quantum states is a major problem in fabricating a working quantum computer. In general the qubit state measurement is destructive. The interaction of a qubit with its environment (e.g., with a charge-sensitive detector) influences the qubit state and usually causes total decoherence. Note, however, that, depending on the mesoscopic system geometry, also partial decoherence can be observed despite the coupling to the environment. Moreover, the energy exchange between the two-state qubit and the qubit meter can occur during the measurement process [1]. Thus for qubit-detector systems the measurement of qubit charge oscillations is usually strongly limited in time.

For a DQD qubit which is capacitively coupled to a quantum point contact (QPC) the state of a charge qubit may be determined [2,3]. The QPC current is sensitive to the two-state qubit occupation and reflects the qubit dynamics. It is also possible to use a single-electron transistor (SET) or a DQD system as a qubit charge meter (detector of the qubit charge) [4–7]. It is interesting that for an asymmetric SET the detector current follows the qubit oscillations, which are distorted much less than in the case of the symmetric SET [6,8]. The DQD meter can also be used to distinguish between qubit states with different electron phases [9]. Instead of DQD detectors one can also use two serially coupled QPCs [10,11].

In this work we present a proposal for a QD wire (QW) between two leads which represents an effective charge qubit meter. We consider theoretically a DQD qubit coupled electrostatically with a single site of a linear chain of QDs. The wire consists of N QD sites and is connected with the left and right electron reservoirs via the tunneling barriers (hopping integrals). In this case the current flowing through the wire is sensitive to the qubit charge oscillations and we treat it as a natural candidate for readout of the two-state system. Additionally, in comparison with a single QD, DQD, or QPC (which are often used in the literature as charge meters), here we analyze a qubit coupled to different wire sites; i.e., we study how a qubit coupled electrostatically with a particular site of the wire influences the qubit decoherence time. We expect that the qubit position on the wire can significantly change the readout current such that long-time measurement of the qubit dynamics is possible.

In order to study qubit dynamics we apply in our calculations the equation of motion (EM) for appropriate correlation functions. This method allows us to obtain all currents flowing in the system as well as the qubit and wire electron occupations. The higher-order correlation functions which appear in the calculations are decoupled beyond the mean-field approximation such that the term which depends on the lead electron annihilation and creation operators taken at the initial time ($t = 0$; all parts of the system are decoupled) is decoupled from the remaining part of the correlation function, which depends on the QD operators taken at a given nonzero time, $t > 0$. This procedure is better than the so-called Hubbard I approximation used in the analysis of the time-independent Hubbard model [12] and was successfully used to describe the dynamics of a qubit coupled with a single QD detector and others [5,13] (see also Ref. [14]). However, for a large number of sites in the wire this method is very cumbersome, thus, for longer wires we apply the evolution operator technique and the mean-field approximation [15,16]. In general, a mean-field treatment should give, for many purposes, a relatively good description of the system. The qualitative comparison of the transient currents in a T-shaped QD system (or in the case of a single impurity coupled with two leads) obtained within the Hartree-Fock (HF) approximation and using other methods (beyond the HF) is satisfactory [17,18] (however, see Ref. [19]). The HF approximation was also successfully applied to describe, e.g., the Anderson impurity [20], the Fano effect [21], the 0.7 anomaly [22], and photon-assisted electron transport through an interacting QD system [23,24]. This approach is very often used due to its simplicity, which allows us to find analytical solutions for the stationary transport as well as for time-dependent phenomena. Note that other time-dependent methods (due to the many-body interactions) are

*tomasz.kwapinski@umcs.pl
†ryszard.taranko@umcs.pl

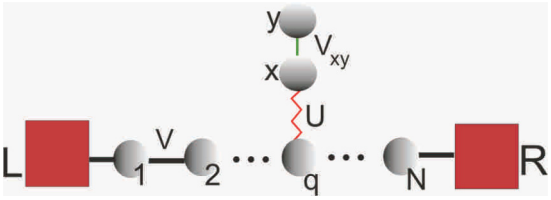

FIG. 1. (Color online) Schematic view of the wire-qubit system: N-site quantum wire coupled electrostatically (via U parameter) with the qubit (two coupled quantum dots: x and y). V_{xy} and V are hopping integrals between qubit quantum dots and between the nearest-neighbour wire sites, respectively.

often limited to infinite correlations, a low or high source-drain voltage, small coupling parameters, the zero-temperature case, almost decoupled systems, and others [2,4,6,25–32]. In this paper we compare the results for short wires calculated within the HF approach and beyond the mean-field approximation: on a qualitative level the conclusions for both methods are similar.

The paper is organized as follows. In Sec. II the main formulas for the current flowing through the system and charges localized on qubit QDs and on the wire sites are derived within the EM method for appropriate correlation functions and within the evolution operator approach. Numerical results for the considered systems are shown and discussed in Sec. III and the last section, Sec. IV, is devoted to conclusions.

II. THEORETICAL DESCRIPTION

The system we consider here consists of a qubit (which is represented by two coupled QDs) and an N-site regular quantum wire (series of QDs), as sketched in Fig. 1. The qubit is coupled electrostatically with the wire and influences the current flowing between the left and the right electrodes. To describe the qubit dynamics we use the tight-binding Hamiltonian, which can be written as $H = H_0 + V$, where

$$H_0 = \sum_{k,\alpha=L,R} \varepsilon_{\alpha k} c^\dagger_{\alpha k} c_{\alpha k} + \sum_{i=1}^{N} \varepsilon_i c^\dagger_i c_i + \varepsilon_x c^\dagger_x c_x + \varepsilon_y c^\dagger_y c_y + U c^\dagger_x c_x c^\dagger_q c_q, \tag{1}$$

$$V = \sum_k V_{Lk} c^\dagger_{Lk} c_1 + \sum_k V_{Rk} c^\dagger_{Rk} c_N + \sum_{i=1}^{N-1} V c^\dagger_i c_{i+1} + V_{xy} c^\dagger_x c_y + \text{H.c.} \tag{2}$$

The operators $c_{\alpha k}(c^\dagger_{\alpha k})$, $c_i(c^\dagger_i)$, $c_x(c^\dagger_x)$, and $c_y(c^\dagger_y)$ are the electron annihilation (creation) operators for the electrode α ($\alpha = L,R$), for the ith wire site or for the first (nearby) and the second (far-removed) qubit QDs, respectively. The electrostatic coupling between the first qubit QD and the q-wire site is described by the parameter U. The first (last) wire site is coupled to the left (right) lead through the tunneling barriers with the transfer-matrix element V_{Lk} (V_{Rk}), and the V and V_{xy} parameters describe the tunnel barriers between the nearest-neighbor wire sites and between both qubit QDs, respectively. Electron-electron on-site Coulomb interactions are neglected in our system (one electron on the qubit and nonmagnetic wire are considered).

In the following we calculate the qubit QD occupations and the current flowing through the multi-QD detector. For a short chain of detector QDs, $N = 1,2,3$, we apply the EM method for some correlation functions and truncate the corresponding higher-order functions one or two orders beyond the mean-field level [5,13,14]. As the application of this method to the detector of longer chains is a rather cumbersome task, for $N \geqslant 4$ (and only for qualitative consideration) the qubit-detector Coulomb interaction is considered within the mean-field treatment. The comparison of these two approximations for $N = 3$ justifies our approach to the subject in question.

A. Beyond the mean-field approximation

The electron current flowing from the αth electrode can be obtained from the time evolution of the occupation number operator of this electrode (expressed in the Heisenberg representation) and takes the form (e.g., Ref. [33]):

$$j_\alpha(t) = 2\,\mathrm{Im} \sum_k V_{\alpha k} \langle c^\dagger_{i'}(t) c_{\alpha k}(t) \rangle, \tag{3}$$

where $\langle \cdots \rangle$ denotes the quantum-mechanical average and $e = \hbar = 1$ units were used. Here, the index i' identifies the QD coupled with the αth lead, i.e., $i' = 1$ for $\alpha = L$ and $i' = N$ for $\alpha = R$. Using the explicit time dependence of $c_{\alpha k}(t)$ obtained by solving the corresponding EM for this operator, Eq. (3) can be rewritten (in the wide-band limit [33]) in the form [5,13,14,33,34]

$$j_\alpha(t) = 2\,\mathrm{Im} \left(\sum_k V_{k\alpha} e^{-i\varepsilon_{\alpha k}} \langle c^\dagger_{i'}(t) c_{\alpha k}(t_0) \rangle - i \frac{\Gamma_\alpha}{2} \langle n_{i'}(t) \rangle \right), \tag{4}$$

where $\Gamma_\alpha = 2\pi \sum_k |V_{k\alpha}|^2 \delta(E - \varepsilon_{\alpha k})$ and we further assume the initial time $t_0 = 0$.

To calculate the current $j_\alpha(t)$ we should know the correlation functions $\langle c^\dagger_i(t) c_{\alpha k}(0) \rangle$ and the occupancy of the ith QD, $\langle n_i(t) \rangle \equiv n_i(t)$. We find these functions by solving the EM for them. It is known that in the EM method one usually obtains an infinite set of coupled equations for correlation functions of higher and higher order (or Green's functions). For example, for $n_1(t)$ we have the following equation:

$$\frac{\partial}{\partial t} n_1(t) = 2\,\mathrm{Im} \left\{ \sum_k V_{Lk} e^{-i\varepsilon_{Lk}} \langle c^\dagger_1(t) c_{Lk}(0) \rangle + V \langle c^\dagger_1(t) c_2(t) \rangle - i \frac{\Gamma_L}{2} n_1(t) \right\}. \tag{5}$$

In the above equation two types of new functions appear, $\langle c^\dagger_1(t) c_2(t) \rangle$ and $\langle c^\dagger_1(t) c_{Lk}(0) \rangle$, for which the corresponding EM should be written. Functions of the first type are the quantum-mechanical averages of different products of the QD electron operators taken at the given time t. Functions of the second type are related to the products of the QD operators taken at time t and leads electron operators taken at initial time $t = 0$. Writing down the EM for $\langle c^\dagger_1(t) c_2(t) \rangle$ and for new functions of the first type, $\langle f_1(a^\dagger_i(t), a_j(t)) \rangle$, which appear in subsequent equations, we obtain closed sets of 8 (for $N = 1$), 15 (for $N = 2$) and 47 (for $N = 3$)

differential equations for them. The functions $\langle f_1(a_i^\dagger(t),a_j(t))\rangle$, e.g., for $N=3$ ($x=4$, $y=5$), are as follows: n_i, $\langle n_i n_j\rangle$, $\langle n_i n_j n_l\rangle$ $(i,j,l=1,2,3,4)$, $\langle n_1 n_2 n_3 n_4\rangle$, $\langle c_1^\dagger c_2\rangle$, $\langle c_1^\dagger c_2 c_4^\dagger c_5\rangle$, $\langle c_2^\dagger c_3 c_4^\dagger c_5 n_1\rangle, \ldots$ (for brevity, here we have omitted the time dependence of all operators). However, this closed (in relation to $\langle f_1(a_i^\dagger(t)a_j(t))\rangle$) set of equations contains 40 sums like $\sum_k V_{\alpha k} e^{-i\varepsilon_{\alpha k}t}\langle f_2(a_i^\dagger(t),a_j(t))c_{\alpha k}(0)\rangle$, where $f_2(a^\dagger,a)$ are the given products of the corresponding QD electron annihilation and creation operators (not shown here). Unfortunately, the corresponding set of equations for $\langle f_2(a_i^\dagger(t),a_j(t))c_{\alpha k}(0)\rangle$ cannot be closed and some approximations should be done. Here we have used the following procedure: (i) the EMs for $\langle f_2(a_i^\dagger(t),a_j(t))c_{\alpha k}(0)\rangle$ are obtained; (ii) the exact solution for $c_{\alpha k}(t)$ is inserted into the equations obtained from (i); (iii) the wide-band limit approximation is used; and (iv) the next higher-order functions are approximated according to the formulas

$$\begin{aligned}&\left\langle f_3(a_i^\dagger(t),a_j(t))c_{\alpha k_1}^\dagger(0)c_{\beta k_2}(0)\right\rangle\\ &\quad\simeq \langle f_3(a_i^\dagger(t),a_j(t))\rangle\left\langle c_{\alpha k_1}^\dagger(0)c_{\beta k_2}(0)\right\rangle\\ &\quad= \langle f_3(a_i^\dagger(t),a_j(t))\rangle\left\langle n_{\alpha k_1}(0)\right\rangle\delta_{\alpha\beta}\delta_{k_1k_2}\end{aligned}\tag{6}$$

and

$$\begin{aligned}&\left\langle f_3(a_i^\dagger(t),a_j(t))c_{\alpha k_1}(0)c_{\beta k_2}(0)\right\rangle\\ &\quad=\left\langle f_3(a_i^\dagger(t),a_j(t))c_{\alpha k_1}^\dagger(0)c_{\beta k_2}^\dagger(0)\right\rangle\simeq 0.\end{aligned}\tag{7}$$

Finally, for $N=3$ we obtain a closed set of 47 differential equations for $\langle f_1(a^\dagger,a)\rangle$ coupled with 122 (for every k vector) equations for $\langle f_4(a_i^\dagger(t),a_j(t))c_{\alpha k}(0)\rangle$. Here, $f_3(a^\dagger,a)$ and $f_4(a^\dagger,a)$ functions are the given products of the QD electron annihilation and creation operators, and, for example, f_4 includes the following terms: $c_1^\dagger$, $c_2^\dagger$, $c_3^\dagger$, $c_1^\dagger n_4$, $c_1^\dagger c_4^\dagger c_5 n_2$, $c_1^\dagger c_2^\dagger c_3 c_4^\dagger c_5$, $c_2^\dagger c_4 c_5^\dagger n_1 n_3, \ldots$ (here, again, for brevity the time dependence of all operators has been omitted). Note that for larger N's ($N>3$) one has to resolve the EM for longer products of $c^\dagger$ and c operators, which is a very arduous procedure and leads to a huge number of differential equations. Thus, using this method we concentrate on rather short QD wires, i.e., for $N<4$.

Note that during calculations of the QD occupations or the current flowing out of or into the left and right leads, we also obtain information on the currents $j_{ij}(t)$ flowing between given neighboring ith and jth QDs:

$$j_{ij}(t)=-2\,\mathrm{Im}\,V_{ij}\langle c_i^\dagger(t)c_j(t)\rangle.\tag{8}$$

Although measurement of these currents is difficult (and beyond the possibilities of most experimental setups), knowledge on the dynamics of the current flowing between different wire sites may be very useful for understanding the electron transport in such systems.

B. Mean-field treatment

In order to study the qubit dynamics for longer wires we apply the HF approximation, which allows us to simplify the many-body Hamiltonian to a single-particle one with the effective on-site electron energies $\varepsilon_x\to\varepsilon_x+Un_q$ and $\varepsilon_q\to\varepsilon_q+Un_x$. The HF approach can be a reliable approximation, as the Coulomb interaction in many quantum structures is small compared with other energies of the system, thus noninteracting eigenstates of the quantum structure are related to those of small U. For the case of large U (if we are not interested in, e.g., the Kondo effect or other many-body complex effects), one can focus on a single Coulomb peak. The EM method does not need decoupling procedures, however, it is difficult to find the general form of the differential equations for the corresponding correlation functions for arbitrary N and q. To resolve this problem we use the evolution operator technique [15,16,35], which allows us to find the current flowing through the system, $j_L(t)=-edn_L(t)/dt$ $[n_L(t)=\sum_{Lk}n_{Lk}(t)]$, as well as the QD occupations, $n_\beta(t)=\sum_{\beta'}n_{\beta'}(t_0)|U_{\beta,\beta'}(t,t_0)|^2$ $(\beta,\beta'=x,y,i,k)$, from our knowledge of the appropriate evolution operator matrix elements $U_{\beta,\beta'}(t,t_0)$. The evolution operator satisfies the general relation (in the interaction representation)

$$i\frac{\partial}{\partial t}U(t,t_0)=\tilde V(t)\,U(t,t_0),\tag{9}$$

where $\tilde V(t)=U_0(t,t_0)V(t)U_0^\dagger(t,t_0)$, $U_0(t,t_0)=T\exp(i\int_{t_0}^t dt'\,H_0(t'))$, and $n_\beta(t_0)$ represents the initial filling of the corresponding single-particle states. Using the above relations for the evolution operator elements, the following differential equations for $U_{Lk,\beta}(t,t_0)$, which are needed to obtain the current, can be written:

$$i\frac{\partial}{\partial t}U_{Lk,\beta}(t,t_0)=\tilde V_{Lk,1}(t)U_{1,\beta}(t,t_0),\tag{10}$$

where nonzero elements of the function $\tilde V_{Lk,1}$ are

$$\tilde V_{1,Lk}(t)=\tilde V_{Lk,1}^*(t)=V_{Lk}^*e^{i(\varepsilon_1-\varepsilon_{Lk})t}e^{iU\delta_{1,q}\int_{t_x}^t n_x(t')dt'}.\tag{11}$$

Here, as before, we assume that $t_0=0$ (at time t_0 all hopping integrals in the wire are switched on) and t_x corresponds to a specific time when the tunneling between the qubit QDs is switched on. To shorten the notation we assume that $U_{\alpha,\beta}(t,t_0)\equiv U_{\alpha,\beta}(t)$. Using the wide-band-limit approximation the time-dependent current takes the form

$$j_L(t)=-\Gamma_L n_1(t)-2\,\mathrm{Im}\left(\sum_{Lk}n_{Lk}(0)\tilde V_{Lk,1}(t)U_{1,Lk}(t)\right).\tag{12}$$

The knowledge of the matrix elements $U_{1,\beta}$ [needed to obtain $n_1(t)$ occupation] and $U_{x,\beta}$ [needed to obtain $n_x(t)$, which also appears in Eq. (11)] allows us to derive the current, Eq. (12). Using Eq. (9) one can write the following set of differential equations for the appropriate elements of the evolution operator:

$$\begin{aligned}\frac{\partial}{\partial t}U_{i,\beta}(t)=&-i\tilde V_{i,i+1}(t)U_{i+1,\beta}(t)-i\tilde V_{i,i-1}(t)U_{i-1,\beta}(t)\\&-i(\delta_{i,1}\delta_{\beta,Lk}+\delta_{i,N}\delta_{\beta,Rk})\tilde V_{i,\beta}(t)\\&-\delta_{i,1}\Gamma_L U_{1,\beta}(t)/2-\delta_{i,N}\Gamma_R U_{N,\beta}(t)/2,\end{aligned}\tag{13}$$

$$\frac{\partial}{\partial t}U_{x(y),\beta}(t)=-i\tilde V_{x(y),y(x)}(t)U_{y(x),\beta}(t),\tag{14}$$

where we assume the same electron energies in all wire QDs, i.e., $\varepsilon_i=\varepsilon_0$ $(i=1,\ldots,N)$. The elements $\tilde V$ in the above

relations read

$$\tilde{V}_{i,j}(t) = \tilde{V}^{*}_{j,i}(t) = V(\delta_{i+1,j} + \delta_{i-1,j}) e^{iU(\delta_{i,q} - \delta_{j,q}) \int_{t_x}^{t} n_x(t')dt'}, \tag{15}$$

$$\tilde{V}_{x,y}(t) = \tilde{V}^{*}_{y,x}(t) = V_{xy} e^{i(\varepsilon_x - \varepsilon_y)t} e^{iU \int_{t_x}^{t} n_q(t')dt'}. \tag{16}$$

From the above set of differential equations one can obtain all quantum wire and qubit QDs occupations, as well as the current flowing through the system. Note that all equations for $U_{\beta,\beta'}(t)$ elements and the occupations $n_\beta(t)$ are coupled to each other, i.e., to obtain the occupation of the nearby qubit QD, $n_x(t)$, we have to know the $U_{x,\beta}(t)$ elements [Eq. (14)]; in Eq. (14) there is a $\tilde{V}_{x,y}$ function which should be obtained for a given q-site occupation, $n_q(t)$. This occupation is obtained from the $U_{i,\beta}(t)$ elements, Eq. (13) [the set of differential equations, Eqs. (13) and (14), is coupled via $n_x(t)$ and $n_q(t)$, which appear in $\tilde{V}_{x,y}$ and $\tilde{V}_{i,\beta}$]. Moreover, to find the solution for the evolution operator elements as a function of time, t, it is necessary to know the charge occupations of $n_q(t')$ and $n_x(t')$ for all t' in the range of $t_x < t' < t$.

As an example, we consider a DQD qubit coupled electrostatically to the meter represented by a single QD placed between two leads, $N = 1$. In this case the evolution operator matrix elements which are required to describe the qubit dynamics can be reduced to simpler forms, and under certain conditions they can be obtained analytically. In particular, one can find that the following elements tend to 0 for large t (i.e., beyond the transient effects): $U_{1,1}(t)$, $U_{1,x/y}(t)$, $U_{x/y,1}(t)$, $U_{x/y,Lk}(t)$, and $U_{x/y,Rk}(t)$. These elements can be omitted in calculations, as they play the role only for small t ($t \geqslant t_0$), and thus the expression, for example, for the occupation of the nearby qubit QD, $n_x(t)$, can be expressed as

$$n_x(t) = n_x(0)|U_{x,x}(t)|^2 + n_y(0)|U_{x,y}(t)|^2, \tag{17}$$

where the evolution operator matrix elements satisfy Eq. (14). One can write a similar equation for $n_y(t)$.

Note that the analytical expression for current flowing through the system can be obtained for the case of vanishing electrostatic coupling U (there is no wire-qubit connection) and for the zero-temperature case. Also, for the case of small U one can obtain the current analytically, as in this case the solution for $U_{1,Lk}(t)$,

$$U_{1,Lk}(t) = -iV_{Lk} e^{-\Gamma t} \int_0^t dt' \exp\left(i(\varepsilon_0 - \varepsilon_{Lk} - i\Gamma)t' + iU \int_{t_x}^{t'} dt'' n_x(t'') \right), \tag{18}$$

can be approximated by (for $t_x = 0$) [23]

$$U_{1,Lk}(t) = -V_{Lk} \frac{\exp\{it[\varepsilon_0 - \varepsilon_{Lk} + Un_x(t)]\}}{\varepsilon_0 - \varepsilon_{Lk} + Un_x(t) - i\Gamma}. \tag{19}$$

Finally, one can find the relation for the current flowing from the left electrode,

$$j_L(t) = \frac{\Gamma}{2\pi} \left(\arctan \frac{\varepsilon_0 - \mu_R + Un_x(t)}{\Gamma} - \arctan \frac{\varepsilon_0 - \mu_L + Un_x(t)}{\Gamma} \right), \tag{20}$$

and the charge accumulated at the detector site,

$$n_1(t) = \frac{1}{2\pi} \left(\pi - \arctan \frac{\varepsilon_0 - \mu_R + Un_x(t)}{\Gamma} - \arctan \frac{\varepsilon_0 - \mu_L + Un_x(t)}{\Gamma} \right). \tag{21}$$

The above analytical solutions (derived for the qubit-QD system) are similar to the results obtained for a single QD between two leads in the stationary case [33]. It is easy to show that for $\varepsilon_0 \to -\infty$ ($\varepsilon_0 \to +\infty$) the occupation of the wire site is maximal (minimal). Note that although the above relations seem not to be complicated, one has to know the time dependence of the qubit occupation $n_x(t)$ (for which we have no simple analytical solution). For a longer QW detector coupled with a DQD qubit, analytical formulas for the charge or the time-dependent current flowing through the wire do not exist because in general the elements $U_{1,Lk}(t)$ are not equal to $U_{N,Rk}(t)$ [36].

III. RESULTS AND DISCUSSION

In this section we show numerical results for the time-dependent current flowing through the wire and occupations of the qubit and wire sites. In our calculations we assume the energy unit $\Gamma = 1$, $\Gamma_L = \Gamma_R = \Gamma$, and symmetrical chemical potentials, $\mu_L = -\mu_R$. Thus the reference energy point (called the Fermi energy of the wire) is $E_F = 0$. Moreover, in order to avoid multilevel quantum interference effects, we concentrate on the transport through a single molecular state of the system; i.e., a regime of small chemical potentials is assumed, $\mu_L = -\mu_R = 1$. The current (time) is expressed in units of $2e\Gamma/\hbar$ ($\hbar/\Gamma$) and the zero-temperature case is considered. Note that one excess electron on the DQD qubit is assumed. In our calculations the qubit is "switched on" at time $t = t_x = 10$ when the detector is already in a stationary nonequilibrium state (all parts of the detector were coupled together at $t_0 = 0$). In other words, we assume that for $t < t_x$ the qubit-wire system is decoupled ($V_{xy} = 0$), and in that case only the far-removed qubit QD is occupied, $n_y(t < t_x) = 1$, $n_x(t < t_x) = 0$. For larger t ($t > t_x$) the qubit occupations (n_x and n_y) change and influence the readout current flowing through the wire.

A. Qubit dynamics for an *N*-site wire

The role of the wire length in the qubit dynamics is examined in Fig. 2, where we show the nearby qubit QD occupation as a function of time for the wire lengths $N = 1, 2$, and 3. Note that different qubit-wire connections and couplings are considered (see inset pictures). For $N = 1$ ($q = 1$; upper solid line) one observes that the qubit QD occupation oscillates in time but these oscillations vanish very rapidly (which is in accordance with the previous literature results, e.g., Ref. [5]). In this case the measurement of the qubit dynamics is limited in time. For $N = 2$ and a qubit coupled with the first or the second wire site, $q = 1$ or $q = 2$ (dotted curves), the situation is similar but the charge oscillations hold somewhat longer than for $N = 1$. The most interesting case is observed for the wire consisting of three sites, $N = 3$ (bottom three curves). Here for the qubit coupled with the first or with the third wire sites, the oscillations of n_x vanish very rapidly. However, for

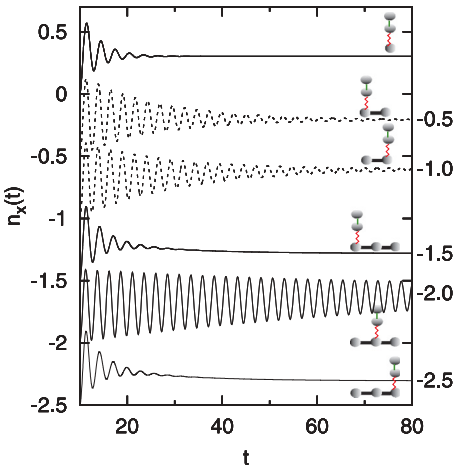

FIG. 2. (Color online) Nearby qubit QD occupations, $n_x(t)$, as a function of time for different qubit-wire connections indicated schematically in the inset pictures (curves, from top to bottom): $N = q = 1$; $N = 2$, $q = 1$; $N = 2$, $q = 2$; $N = 3$, $q = 1$; $N = 3$, $q = 2$; and $N = 3$, $q = 3$. The other parameters are $V = 4$, $V_{xy} = 1$, $U = 4$, $\varepsilon_0 = \varepsilon_x = \varepsilon_y = 0$, $\mu_L = -\mu_R = 1$, $t_0 = 0$, $t_x = 10$, and $\Gamma_L = \Gamma_R = 1$. The curves, from top to bottom, are shifted by 0, -0.5, -1.0, -1.5, -2.0, and -2.5, respectively, for better visualization. The unit of time (energy) is $\hbar/\Gamma$ (Γ).

$q = 2$ (qubit coupled with the second wire site), the nearby qubit QD oscillations hold even for longer t and disappear very slowly. To explain this interesting effect, in Sec. III B we consider the local density of states (LDOS) on the wire sites and the time evolution (phase behavior) of the current and the qubit occupation.

B. Readout current oscillations

In Sec. III A we have shown that for a specific qubit-wire connection the nearby qubit QD occupation oscillates for a very long time. We expect that this behavior should also be reflected in the readout current flowing through the wire. To corroborate this effect we study the current flowing from the left electrode to the three-site wire (Fig. 3, upper panel). The qubit is coupled with the first wire site ($q = 1$, dotted curves) or with the second one ($q = 2$, solid curves). As one can see, in comparison with the case of $q = 1$, the current oscillations for $q = 2$ hold for a longer t, which is in accordance with the results depicted in Fig. 2. Thus, the qubit dynamics strongly depends on the qubit position (connection) along the wire and, more importantly, on the total number of wire sites. This effect is related to the wire DOS. For $U = 0$ and for an odd (even) number of sites in the wire the system is characterized by a high (low) value of the total DOS; in other words, there is one molecular state at the Fermi energy $E = \varepsilon_0 = E_F$. However, the LDOS (at the Fermi level) changes along the wire, and, e.g., for $N = 3$ there is a high value of the LDOS on the first and third sites, while for the second (middle) site the LDOS is very low. The structure of the LDOS determines the wire conductance, and, e.g., for $N = 2$, electrons do not flow through the wire (for a low source-drain voltage), but for $N = 3$ the conductance is maximal [37]. We have found that the readout current oscillations do not vanish very rapidly

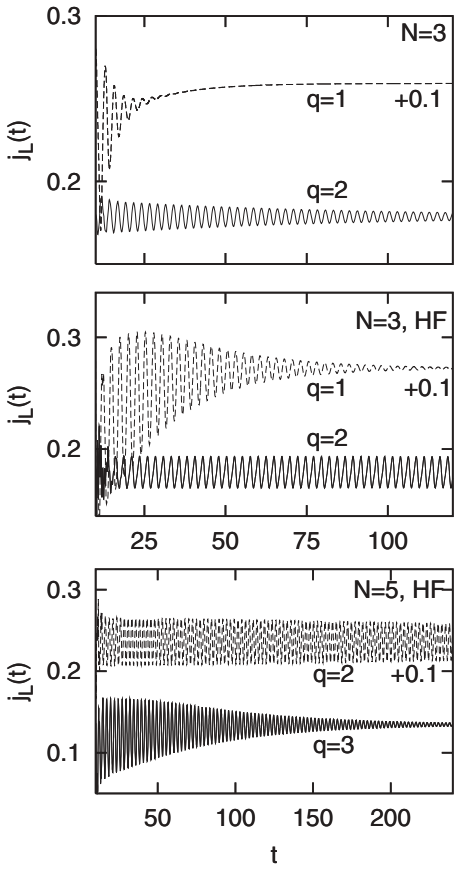

FIG. 3. Upper panel: Current flowing from the left electrode for the wire length $N = 3$ and for a qubit coupled to the first wire site, $q = 1$, or to the middle site, $q = 2$. Middle panel: The same results as in the upper panel but obtained within the HF approximation. Bottom panel: Current flowing through the five-site wire depicted for two qubit-wire connections: $q = 2$ and $q = 3$ (HF approximation). Other parameters are the same as in Fig. 2. The curves for $q = 1$ are shifted by $+0.1$ for better visualization. The unit of current (time, energy) is $2e\Gamma/\hbar$ ($\hbar/\Gamma$, Γ).

if two conditions are satisfied: (i) the conductance through the wire is maximal, i.e., electrons can easily flow through the wire sites (the current signal is high); and (ii) the qubit is coupled with a wire site which is characterized by a very low LDOS at the Fermi level. The latter is crucial to obtain long-time oscillations: in that case the qubit and the wire states do not overlap and thus the system needs a longer time to obtain its stationary state. If the wire site is characterized by a high value of the LDOS at the Fermi level, then the energy exchange between the two subsystems is more effective and the measurement of the readout current oscillations is strongly limited in time. Note that for $U \neq 0$ the energy of the molecular states of the wire-qubit system can differ somewhat from that for the isolated wire. However, we expect that our explanation will remain valid.

In order to generalize our conclusions we should perform calculations of the readout current also for longer wires. Unfortunately, in general, the EM method for the required functions cannot be easily applied to large N's and we decided to use the evolution operator method together with the HF approximation (discussed in Sec. II B). First, we compare the

results obtained within the HF method (Fig. 3, middle panel) with those shown in the upper panel in Fig. 3 (calculations done beyond the mean-field approximation). As one can see, the HF method applied for the case of $N = 3$ gives the same qualitative results (for larger t) as the mean-field treatment does. Both approaches indicate vanishing current oscillations for $q = 1$ and long-lived oscillations for $q = 2$. Of course, the decay time of the current oscillations is longer for the HF case but this behavior is not surprising because the mean-field approximation often overestimates the obtained values.

As the qualitative results shown in the upper two panels in Fig. 3 are satisfactory, for further qualitative discussion we calculate within the evolution operator method and the HF approximation the readout current flowing through an $N = 5$ site wire with the qubit coupled to the second site, $q = 2$, and to the middle one, $q = 3$; the results are shown in the bottom panel in Fig. 3. Note that for $N = 5$ (odd number of sites) the wire conductance is maximal [37], thus the first condition on the long-time oscillations is satisfied. Moreover, the first, the third, and the fifth wire sites possess a peak in the LDOS at the Fermi level, while the second and the fourth sites have no LDOS peaks at E_F. Thus if the qubit is coupled with the second wire site (low LDOS value at E_F), we expect long oscillations of the readout current. This prediction is confirmed in the bottom panel in Fig. 3, for $q = 2$. On the other hand, for $q = 3$ (nonzero LDOS at the Fermi level) the current oscillations vanish much more rapidly than for the case of $q = 2$ (Fig. 3, bottom panel), which is in accordance with the results shown in the upper panel for $N = 3$.

In order to investigate further the role of the qubit-wire geometry (connection to different wire QDs) in the readout current, we focus on the inside currents flowing between the wire sites, Eq. (8). Thus for a wire consisting of $N = 3$ sites we compare the left and the right currents flowing from and into the electrodes and the currents j_{12} and j_{23} flowing between the first and the second sites or between the second and the third sites, respectively. All mentioned currents for the qubit coupled with the first, $q = 1$ (second, $q = 2$), wire QD are depicted in Fig. 4, upper panel (bottom panel). As one can see, there are no common features of the two cases. For $q = 1$ the oscillations of the left and right currents vanish very rapidly in time but they are out of phase (not in-phase and not in antiphase) in relation to each other. The situation for $q = 2$ is different. The minima of the left current correlate with the maximal values of the right current (both currents oscillate longer in time than for the case of $q = 1$). More interesting behavior holds for the inside wire currents. For $q = 1$ (Fig. 4, upper panel) the currents j_{12} and j_{23} are almost the same and there is no phase difference between them. This means that the middle wire site does not change the current phase; i.e., the occupation of this site is almost constant and does not oscillate in time (not shown here). However, for $q = 2$ (Fig. 4, bottom panel) the qubit is coupled to the middle wire site and the inside wire currents j_{12} and j_{23} oscillate "in antiphase" (the minima of j_{12} correspond to the maxima of j_{23}). In this case the current oscillations do not vanish very rapidly, as the system stays in a kind of resonance mode (antiphase oscillations of the inside currents).

It is also interesting to study the phase shift between the readout current and the qubit occupation (if they are in-phase, in antiphase, or out of phase). Thus in the upper panel in

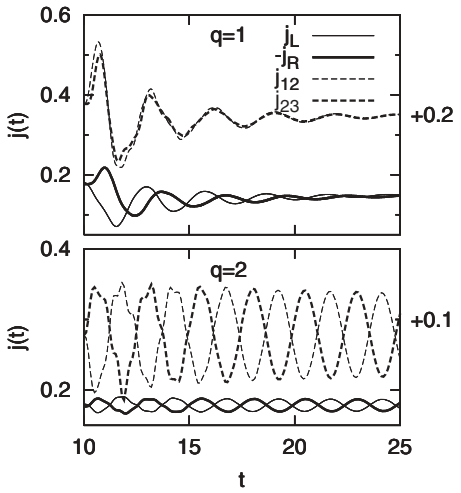

FIG. 4. Current flowing from the left and right electrodes, j_L and j_R (thin and thick solid lines, respectively), and flowing between wire sites j_{12} and j_{23} (thin and thick dotted curves, respectively), for the wire length $N = 3$ and a qubit coupled to the first wire site, $q = 1$ (upper panel), or to the second one, $q = 2$ (bottom panel). Other parameters are the same as in Fig. 2. Dotted curves are shifted by 0.2 or 0.1 for better visualization.

Fig. 5 we analyze the left current oscillations for $N = 3$ (solid curves) and compare them with the nearby qubit QD occupation, n_x (dashed curves; to compare the phase shift they are not plotted in scale). As one can see, the current j_L and the occupation n_x are exactly in antiphase for the case of $q = 1$. This means that for a maximal value of the nearby qubit QD occupation, the current flowing from the left electrode to the wire is characterized by a local minimum (which seems

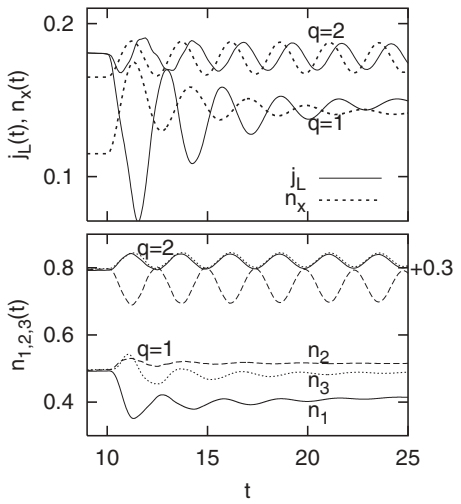

FIG. 5. Upper panel: Current flowing from the left electrode as a function of time for the wire length $N = 3$ and for $q = 1$ and $q = 2$ (solid lines; the same as in Fig. 4) and the nearby qubit QD occupations (dotted curves). For easier comparison of the $n_x(t)$ and $j_L(t)$ phases, the occupation curve for $q = 2$ ($q = 1$) was divided by 25 (10) and shifted by +0.165 (+0.115). Bottom panel: Occupations of the wire sites $n_1(t)$, $n_2(t)$, and $n_3(t)$ for $q = 1$ and $q = 2$, respectively. The curves for $q = 2$ are shifted by +0.3 for better visualization. Other parameters are the same as in Fig. 2.

quite reasonable). However, for $q = 2$ the current oscillations are not in-phase and not in antiphase with the nearby qubit QD occupations, n_x. Thus for a given value of t the left current increases and at the same time the occupation of the nearby qubit QD increases (in the first stage), but then it starts to decrease. This leads to hardly vanishing current oscillations. We have found that the phase shift between the current and the qubit oscillations depends on the number of QW sites between the lead and the site which is connected to the qubit. These sites stand for a kind of a buffer for electrons flowing through the system and can change the current phase in comparison with the qubit charge oscillations. The results shown in Fig. 5 indicate that the qubit lost its coherence more rapidly for a perfect antiphase compatibility between the current and the qubit occupation (the case of $q = 1$; Fig. 5, upper panel). Next, it is desirable to analyze the occupancies of the wire sites for both qubit-wire configurations, i.e., for $q = 1$ and $q = 2$. As one can see in the bottom panel in Fig. 5, all QW sites for the decoupled qubit-wire systems (for $t < 10$) are almost half-occupied, $n_1 = n_2 = n_3 = 0.5$, as here we consider symmetrical couplings to the leads and low source-drain voltages. Note, however, that for asymmetrically coupled systems and high bias voltages the occupations of all sites can be very different, as, e.g., in the DQD system discussed in Ref. [6]. For such systems coupled with a qubit the electron occupations at the QD sites determine the decoherence time; decoherence is suppressed when the qubit is coupled with low-occupied sites [6,38]. It is important that in our system all wire sites have the same occupancies for $U = 0$. Thus the detector occupancy cannot be responsible for the different time decoherences and we explain this effect using the LDOS for the wire sites together with the phase-shift arguments. For nonzero U we observe quite different behavior of the qubit dynamics for the considered configurations ($q = 1$, $q = 2$). In the presence of the qubit-wire coupling ($t > 10$) the occupancies of the wire sites oscillate in time much longer for $q = 2$ than for $q = 1$ but their values do not differ drastically. The lowest occupancies we observe are for the wire site which is coupled to the qubit (due to the qubit-wire electrostatic repulsion), i.e., n_1 for $q = 1$ and n_2 for $q = 2$. It is also interesting that the occupancy oscillations at that site (which is coupled with the qubit) are exactly in antiphase with the oscillations at the rest sites (not coupled with the qubit).

C. Role of the qubit-wire coupling

In order to study the influence of the electrostatic coupling, U, on the qubit oscillations, in Fig. 6 we show the time-dependent charge localized at the nearby qubit QD, $n_x(t)$, for the wire length $N = 3$ and for different values of U (thin lines). The qubit is coupled with the first wire site, $q = 1$ (upper panel), or with the second one, $q = 2$ (bottom panel). For $U = 0$ the qubit is separated from the environment, which leads to undamped electron oscillations between the two qubit QDs. Careful inspection of the results for both qubit-wire connections and nonzero U reveals that the amplitude of the charge oscillations decreases with the qubit-wire coupling. It is also important that the period of the charge oscillations (and also the current oscillations) depends on U and the qubit position on the wire. In general, the period of the

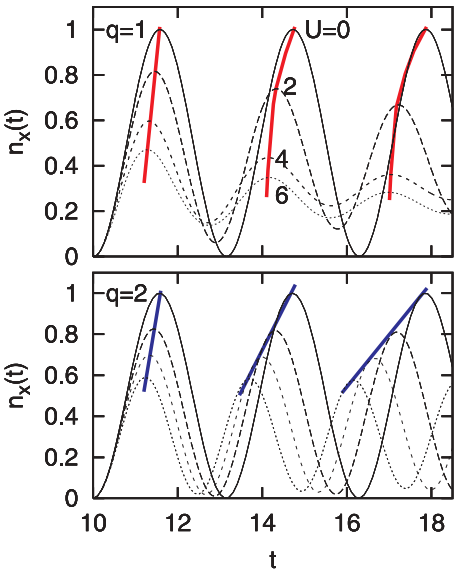

FIG. 6. (Color online) Nearby qubit QD occupations as a function of time for the wire length $N = 3$ and two qubit-wire connections, $q = 1$ (upper panel) and $q = 2$ (bottom panel), for different electrostatic couplings: $U = 0$, 2, 4, and 6. Thick lines indicate the period behavior of the qubit QD occupations. Other parameters are the same as in Fig. 2.

charge oscillations decreases in comparison with the case of a nondisturbed qubit, $U = 0$. This effect, however, depends on the qubit-wire connection; e.g., for $q = 1$ the period of n_x decreases for small U but for larger electrostatic couplings it does not change (see the thick lines in the upper panel in Fig. 6, which tend to a vertical position for larger U). For $q = 2$ the period of the qubit oscillations changes linearly with U (see the thick straight lines in the bottom panel in Fig. 6). Also, the oscillation amplitudes decrease with U in this case, but not as rapidly as for $q = 1$.

D. Nonzero gate voltage regime

The next interesting question is whether the values of the meter on-site energies influence the qubit dynamics. Thus in Fig. 7 we show the current flowing from the left lead as a function of ε_0 ($=\varepsilon_1 = \varepsilon_2 = \varepsilon_3$) and the time for the case of $N = 3$ and $q = 2$ (the qubit is coupled with the middle wire

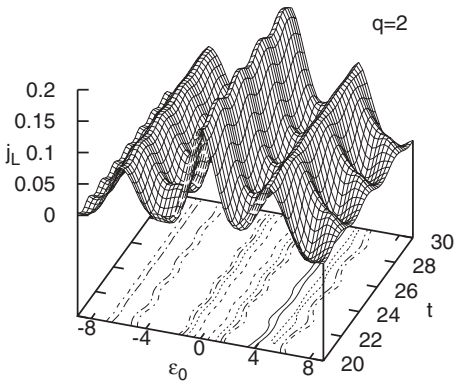

FIG. 7. Current flowing from the left electrode as a function of time and ε_0 for $q = 2$ and $U = 8$. Other parameters are the same as in Fig. 2.

site). For no qubit-wire connection, $U = 0$, the current as a function of ε_0 is characterized by three local maxima, as there are three molecular states of the triple-QD system. For nonzero U these three maxima of $j_L(t)$ as a function of ε_0 are still visible but they are somewhat shifted in comparison with the nondisturbed wire. It is interesting that for $q = 2$ the current is characterized by long-time oscillations for $\varepsilon_0 = 0$ (no LDOS at the Fermi level, which was discussed earlier), but it almost does not oscillate for positive and negative values of ε_0 which correspond to the sideband molecular states (localized at $\varepsilon_0 \simeq \pm 4$). In these cases the qubit is coupled with the wire site which is characterized by a high value of the LDOS at the Fermi energy, and thus, according to our previous results, the readout current oscillations vanish very rapidly in time. For other values of ε_0 the LDOS at the Fermi energy is much lower and the qubit dynamics may be measured for an even longer time (see, e.g., the current oscillations for $\varepsilon_0 \simeq \pm 8$).

IV. CONCLUSIONS

In summary, using the EM method for appropriate correlation functions and the evolution operator technique, time-dependent electron transport through an N-site linear quantum wire coupled electrostatically with a DQD qubit has been investigated. A system is proposed for monitoring the location of an electron in qubit QDs, i.e., to measure the qubit dynamics.

As the main feature of the qubit-wire system we have found that in the regime of low source-drain voltages (single-molecular-state transport), the measurement of the qubit dynamics strongly depends on the number of sites in the wire, N, and the location of the qubit connection with a wire site (qubit-wire geometry). In particular, the long-time oscillations of the readout current hold for a QW detector which is characterized by a high conductance and a low value of the LDOS (on the site coupled with the qubit) at the Fermi level. Thus, e.g., for $N = 3$ and for a qubit coupled with the first or third wire site, the amplitude of the current oscillations decreases very rapidly with time (strong decoherence), while for a qubit coupled with the second wire site the current oscillations hold longer (weak decoherence).

Additionally, we have shown that in the presence of long-time oscillations the readout current and the nearby qubit QD occupation are out of phase, i.e., not in-phase or in antiphase. If these quantities oscillate in antiphase, the measurement of the qubit dynamics is strongly limited in time.

We hope that the results of this paper can be confirmed experimentally and that they will stimulate qubit experiments with a linear QD geometry and such a QD wire turns out to be a more effective qubit dynamics meter.

ACKNOWLEDGMENTS

This work was supported by Grant No. N N202 330 939 (T.K.) and Grant No. N N202 263 138 (R.T., T.K.) from the Polish Ministry of Science and Higher Education.

[1] X. Q. Li, W. K. Zhang, P. Cui, J. Shao, Z. Ma, and Y. J. Yan, Phys. Rev. B **69**, 085315 (2004).
[2] H.-S. Goan, G. J. Milburn, H. M. Wiseman, and H. B. Sun, Phys. Rev. B **63**, 125326 (2001).
[3] S. A. Gurvitz, Phys. Rev. B **56**, 15215 (1997).
[4] T. Tanamoto and X. Hu, Phys. Rev. B **69**, 115301 (2004).
[5] R. Taranko and P. Parafiniuk, Physica E **40**, 2765 (2008).
[6] T. Gilad and S. A. Gurvitz, Phys. Rev. Lett. **97**, 116806 (2006).
[7] H. M. Wiseman, D. W. Utami, H. B. Sun, G. J. Milburn, B. E. Kane, A. Dzurak, and R. G. Clark, Phys. Rev. B **63**, 235308 (2001).
[8] S. A. Gurvitz and G. P. Berman, Phys. Rev. B **72**, 073303 (2005).
[9] Ch. Kreisbeck, F. J. Kaiser, and S. Kohler, Phys. Rev. B **81**, 125404 (2010).
[10] T. Tanamoto and X. Hu, J. Phys.: Condens. Matter **17**, 6895 (2005).
[11] T. Tanamoto, Jpn. J. Appl. Phys. **49**, 04DJ08 (2010).
[12] J. Hubbard, Proc. R. Soc. A **276**, 238 (1963).
[13] P. Parafiniuk and R. Taranko, Acta Phys. Pol. A **116**, 844 (2009).
[14] A. Croy, U. Saalmann, A. R. Hernandez, and C. H. Lewenkopf, Phys. Rev. B **85**, 035309 (2012).
[15] T. B. Grimley, V. C. J. Bhasu, and K. L. Sebastian, Surface Sci. **121**, 305 (1983).
[16] M. Tsukada, Prog. Theor. Phys. Suppl. **106**, 257 (1991).
[17] I. Tifrea, G. Pal, and M. Crisan, Physica E **43**, 1887 (2011).
[18] A.-M. Uimonen, E. Khosravi, A. Stan, G. Stefanucci, S. Kurth, R. van Leeuwen, and E. K. U. Gross, Phys. Rev. B **84**, 115103 (2011).
[19] A.-M. Uimonen, E. Khosravi, G. Stefanucci, S. Kurth, R. van Leeuwen, and E. K. U. Gross, J. Phys. Conf. Ser. **220**, 012018 (2010).
[20] A. C. Hewson, Phys. Rev. **144**, 420 (1966).
[21] D. Sztenkiel and R. Świrkowicz, Physica E **40**, 766 (2008).
[22] C. Sloggett and O. P. Sushkov, Surface Sci. **601**, 5788 (2007).
[23] Q.-f. Sun and T.-h. Lin, J. Phys.: Condens. Matter **9**, 4875 (1998).
[24] T. Kwapiński, R. Taranko, and E. Taranko, Acta Phys. Pol. A **99**, 293 (2001).
[25] S.-H. Ouyang, C.-H. Lam, and J. Q. You, J. Phys.: Condens. Matter **18**, 11551 (2006).
[26] X. Q. Li, J. Luo, Y. G. Yang, P. Cui, and Y. J. Yan, Phys. Rev. B **71**, 205304 (2005).
[27] J. Y. Luo, X. Q. Li, and Y. J. Yan, Phys. Rev. B **76**, 085325 (2007).
[28] X. Q. Li, P. Cui, and Y. J. Yan, Phys. Rev. Lett. **94**, 066803 (2005).
[29] T. M. Stace and S. D. Barrett, Phys. Rev. Lett. **92**, 136802 (2004).
[30] N. P. Oxtoby, H. M. Wiseman, and H.-B. Sun, Phys. Rev. B **74**, 045328 (2006).
[31] C. Gan, P. Huang, and H. Zheng, J. Phys.: Condens. Matter **22**, 115301 (2010).

[32] L. E. F. Foa Torres, C. H. Lewenkopf, and H. M. Pastawski, Phys. Rev. Lett. **91**, 116801 (2003).
[33] A.-P. Jauho, N. S. Wingreen, and Y. Meir, Phys. Rev. B **50**, 5528 (1994).
[34] E. Taranko, M. Wiertel, and R. Taranko, J. Appl. Phys. **111**, 023711 (2012).
[35] R. Taranko, T. Kwapiński, and E. Taranko, Phys. Rev. B **69**, 165306 (2004).
[36] T. Kwapiński, Phys. Rev. B **69**, 153303 (2004); Vacuum **74**, 201 (2004).
[37] T. Kwapiński, J. Phys.: Condens. Matter **17**, 5849 (2005).
[38] Y. Ye, Y. Cao, X.-Q. Li, and S. Gurvitz, Phys. Rev. B **84**, 245311 (2011).